IEEE Access
Multidisciplinary | Rapid Review | Open Access Journal

Received May 29, 2019, accepted June 10, 2019, date of publication June 14, 2019, date of current version July 2, 2019.

Digital Object Identifier 10.1109/ACCESS.2019.2923100

Study on Pressure Transients in Low Pressure Water-Hydraulic Pipelines

DAN JIANG, QIXIA LU, YUANMING LIU, AND DONGDONG ZHAO
School of Mechanical and Electrical Engineering, University of Electronic Science and Technology of China, Chengdu 611731, China

Corresponding author: Dan Jiang (jdan2002@uestc.edu.cn)

This work was supported in part by the National Natural Science Foundation of China under Grant 51205045, Grant 51775089, and Grant 61305092, in part by the Sichuan Science and Technology Program under Grant 2018JY0565, in part by the Fundamental Research Funds for the Central Universities, China, under Grant ZYGX2016J160, and in part by the Open Foundation of the State Key Laboratory of Fluid Power and Mechatronic Systems under Grant GZKF-201515.

ABSTRACT The pressure transients in low pressure water-hydraulic pipelines are worthy of study in hydraulic systems since the frequency-dependent friction model and initial gas bubble volume have generally unknown parameters and lead to unfavorable pressure peaks. More seriously, the transmission efficiency will be significantly reduced. To predict the accurate pressure transients in the water-hydraulic pipelines, a new method is adopted to identify unknown parameters, such as the weighting function coefficients of friction model and the initial gas bubble volume by using the genetic algorithms (GAs). Based on the errors performance between the experimental data and the simulation results, these global optimal parameters are obtained during the water-hydraulic pipeline pressure transients. In the experiments, the pressure pulsations, cavitation and gas bubbles growth, and collapse in the low pressure water-hydraulic pipeline are recorded by two pressure transducers and a high-speed video camera, respectively. Furthermore, the simulation results with respect to the model parameters optimized by the genetic algorithms are consistent with the corresponding experimental data.

INDEX TERMS Water-hydraulic pipelines, pressure transients, frequency-dependent friction, initial gas bubble volume, genetic algorithms.

NOMENCLATURE

c_p	Acoustic velocity in copper pipe;
c_t	Acoustic velocity in tube;
c_0	Acoustic velocity in the fluid;
D_p	Inner diameter of copper pipe;
D_t	Inner diameter of tube;
E_p	Young's modulus of copper;
E_t	Young's modulus of tube;
e_p	Wall thickness of copper pipe;
e_t	Wall thickness of tube;
f	Coefficient of Darcy–Weisbach;
f_f	Fitness function;
F_0	Steady friction;
$F(q)$	Friction;
g	Acceleration due to gravity;
k	Number of weighting terms;
K_{eff}	Effective bulk modulus of fluid;
K_g	Bulk modulus of gas;
K_l	Bulk modulus of liquid;
L	Total length of tested pipe;
L_p	Length of copper pipe;
L_t	Length of tube;
n_i, m_i	Weighting function coefficients of friction;
p	Pressure in pipeline;
p_A, p_B, p_P	Pressure at points A, B, and P;
p_{Lexp}	Experimental pressure transients;
p_{Lss}	Steady-state pressure;
p_{Lth}	Predicted pressure transients;
q	Flow rate in pipeline;
q_A, q_B, q_P	Flow rate at points A, B, and P;
q_2	Inflow rate of an element in the pipe;
q_1	Outflow rate of an element in the pipe;
r_0	Radius of the pipeline;
T_j	Time duration during experimental pressure peaks;
V_{cav}	Cavitation volume;
V_g	Volume of gas bubbles;
V_l	Volume of unit volume of the fluid;

The associate editor coordinating the review of this manuscript and approving it for publication was Zheng Chen.

v_0 Initial velocity in the fluid;
Y_i Weighting function;
α Void fraction;
α_i Initial void fraction;
θ_0 Pipe slope;
ρ_g Density of gas;
ρ_l Density of liquid;
ρ_m Mean density of mixture;
μ_m Mean viscosity of mixture;
τ Dimensionless time.

I. INTRODUCTION

Pressure transients in low pressure water-hydraulic pipelines are common phenomenon in hydraulic systems, which exist in hydraulic suction pipelines and return pipelines with sudden valve closure. Since the pressure transients are accompanied with cavitation and gas bubbles growth and collapse, it leads to an excessive noise, vibration and erosion [1], [2]. Furthermore, the pressure pulsations with uncertain initial gas bubble volume will degrade the transmission efficiency and control performance of electrohydraulic systems [3]–[9]. Due to the pipeline friction and initial gas bubble volume are usually unknown and difficult to be precisely measured in experiment, the pressure transient prediction in low pressure water-hydraulic pipelines is a challenge problem [2]. Although the model construction of the frequency-dependent friction in pipelines has been studied by many authors previously, the parameter identification accuracy and the algorithm robust [10], [11] still need to be further improved to guarantee the model wide adaptability of pressure transients in water-hydraulic pipelines.

Hirose [12] developed a relationship for the turbulent flow with frequency-dependent friction. Suzuki *et al.* [13] adopted weighting function to improve the simulation efficiency of the frequency-dependent friction in a transient laminar flow. Schohl [14] presented a nonlinear least squares approach to approximate the five-terms of the weighting function and improved the transient result performance. Vardy and Brown [15] developed a weighting function model for turbulent flows in a smooth pipeline with moderate Reynolds number. Then Johnston [16] presented the novel friction item that should be concentrated and calculated on the top end of each pipeline to improve the calculation efficiency. Bergant *et al.* [17], [18] investigated parameters that may significantly affect pressure pulsations shape and timing, including unsteady friction, cavitation model and initial void fraction. Ferrari [19] discussed the influence of frequency-dependent friction and the void fraction on the simulation of the pressure wave dynamics. Urbanowicz and Zarzycki [20] and Urbanowicz [21] analyzed expressions for effective weighting functions of unsteady friction during simulation of water hammer. Chaudhry [2] investigated the effects of initial void fraction on density of fluid, acoustic velocity and pressure transients. He also studied the friction model in pipelines. Szymkiewicz and Mitosek [22] presented alternative form of convolution approach to unsteady friction. Jiang *et al.* [23], [24] have already investigated pressure pulsations with cavitation in oil-hydraulic pipelines. Subsequently, Martins *et al.* [25], [26] used a computational fluid dynamics (CFD) model and one-dimensional model together with different unsteady friction formulations (IAB and CB models) to study the low Reynolds number turbulent flows. However, the unknown initial gas bubble volume and the uncertain frequency-dependent friction coefficients will degrade the model identification.

Thanks to the research development of the aforementioned pipeline pressure pulsations, this study is supplied valuable intention. The main contribution of this study is given by

(i) A new parametric identification is presented for the frequency-dependent friction model and initial gas bubble volume by using genetic algorithms to improve the transient pressure performance. The fitness function of the proposed genetic algorithms is described as the total errors of pressure pulsations between the simulation and the corresponding experimental results;

(ii) Meanwhile, to verify the effectiveness of the proposed method, a pressure transient simulation with cavitation and gas bubbles is analyzed. Then the comparative results with Kagama model [27] in water-hydraulic pipelines also verify the consistent performance by both the parametric identification simulation and the corresponding experimental results of transient pressure pulsations.

II. EXPERIMENTAL BENCH DESCRIPTION

By referring to the idea of hammer from Kojima and Shinada [28], the pressure transients are triggered by a steel ball, which is released from an upstream reservoir and hits a valve seat to shut off water flow in a pipeline. Hence, the experimental schematics is shown in Fig. 1, which includes a tested pipeline, a rapid shut-off valve, a reservoir and a centrifugal pump. The rapid shut-off valve consists of coils, a valve seat and the steel ball. The valve seat is wrapped by electrified coils to create magnetic force that prevents the steel ball from rebounding. Due to one-way pump, a centrifugal pump cannot change the flow direction in the test pipeline to make the steel ball travel from the valve seat back to the upstream reservoir for next experimental usage. Here the four ball valves (#1-#4) are used to change the flow direction in the test pipeline. In this experiment, the test pipeline is the suction line of water-hydraulic pump, which is horizontally placed and rigidly installed. This test pipeline is comprised by the copper pipeline and the transparent tube. The corresponding pipeline parameters are listed in Table 1.

The experimental bench of pressure transients is shown in Fig. 2. The upstream reservoir is exposed to local atmosphere and its pressure head is 0.25 m. The centrifugal pump is used to supply constant water flow no more than $5m^3/h$. The flow rate in the experimental pipeline can be regulated by a variable speed electric motor. And a float flowmeter (uncertainty: $\pm 4\%$) is used to measure the initial velocity v_0

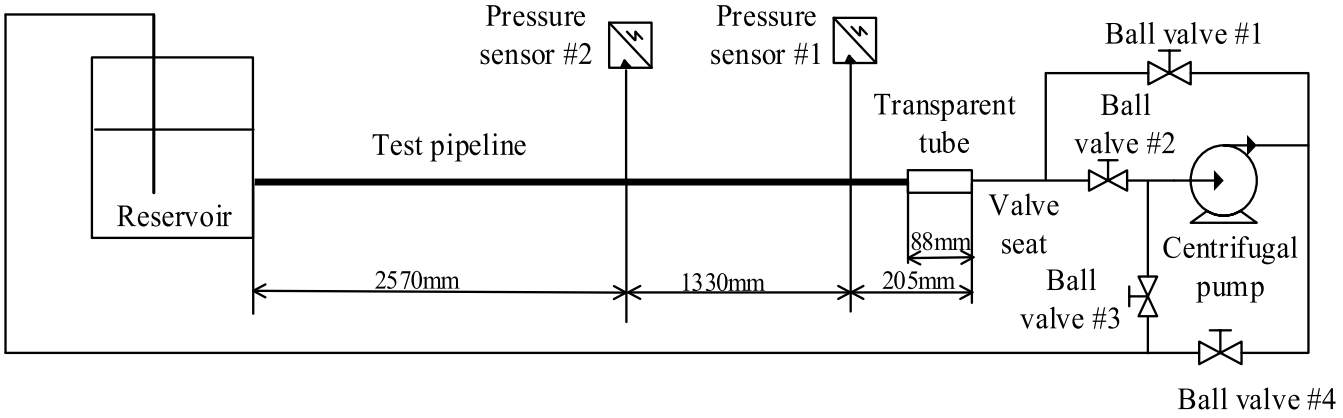

FIGURE 1. The experimental schematics of pressure transients.

TABLE 1. The parameters of copper pipeline and transparent tube.

Variable	Parameters	Values
L_p	Copper pipeline length	4017 mm
D_p	Inner diameter of copper pipeline	16 mm
e_p	Wall thickness of copper pipeline	3 mm
E_p	Young's modulus of copper	120 GPa
L_t	Transparent tube length	88 mm
D_t	Inner diameter of transparent tube	16 mm
e_t	Wall thickness of transparent tube	2 mm
E_t	Young's modulus of transparent tube	4.6 GPa
L	Total length of tested pipeline	4105 mm

in the fluid. The pressure pulsations in the test pipeline are measured by two piezoelectric pressure sensors. Two pressure sensors (pressure range: 0-17 bar, frequency response: >400 kHz, sensitivity: 5 mV/0.017 bar, and uncertainty: ± 0.1%) are installed along the experimental pipeline. One is located near the valve(sensor #1) and the other is in the middle section of the pipeline(sensor #2) as shown in Fig. 1. The measured data is recorded by DAQ board (Advantech PCI-1710HGU) with 20 kHz sample rate. By using a high speed video camera (Lightning RDT^{TM}/16, record rate: up to 5000 frames per second), the growth and collapse of both cavitation and gas bubbles in the transparent tube are obtained during the sudden closure of valve. The transparent viewing tube is glued to the test pipeline, as shown in Fig. 2. The pressure pulsations as well as the visualized cavities, together with gas bubbles growth and collapse are recorded under two different experimental conditions.

III. MATHEMATICAL MODEL CONSTRUCTION

A. BASIC EQUATIONS

As the sudden valve is shut off in the pipeline, the corresponding continuity and motion equations can be described based on mass and momentum conservation laws [1]

$$\frac{1}{{c_0}^2}\frac{\partial p}{\partial t}+\frac{\rho_m}{\pi {r_0}^2}\frac{\partial q}{\partial x}=0, \tag{1}$$

$$\frac{\rho_m}{\pi {r_0}^2}\frac{\partial q}{\partial t}+\frac{\partial p}{\partial x}+F(q)+\rho_m g\sin\theta_0=0. \tag{2}$$

The above mean density ρ_m is given by

$$\rho_m=(1-\alpha)\rho_l+\alpha\rho_g, \tag{3}$$

where the void fraction α is the volume ratio of gas bubbles per unit fluid volume, which yields

$$\alpha=\frac{V_g}{V_l}. \tag{4}$$

Theoretically, the acoustic velocity c_0 is given by [29], [30]

$$c_0=\frac{L_p+L_t}{\frac{L_p}{c_p}+\frac{L_t}{c_t}}, \tag{5}$$

where c_p and c_t are the acoustic velocity in the copper pipe and in the transparent tube respectively, which can be calculated by

$$c_p=\frac{\sqrt{\frac{K_{eff}}{\rho_m}}}{\sqrt{1+\frac{D_pK_{eff}}{e_pE_p}}}, \tag{6}$$

$$c_t=\frac{\sqrt{\frac{K_{eff}}{\rho_m}}}{\sqrt{1+\frac{D_tK_{eff}}{e_tE_t}}}, \tag{7}$$

where K_{eff} is the effective bulk modulus of fluid. It can be calculated by [23] as follow

$$K_{eff}=\frac{K_gK_l}{\alpha(K_l-K_g)+K_g}, \tag{8}$$

where K_g and K_l are the bulk modulus of gas and liquid respectively. Furthermore, K_g is proportional to the pressure in the pipeline p as follow [1]

$$K_g=1.4p. \tag{9}$$

On the other hand, K_l is set to be 2.1×10^9 Pa for water.

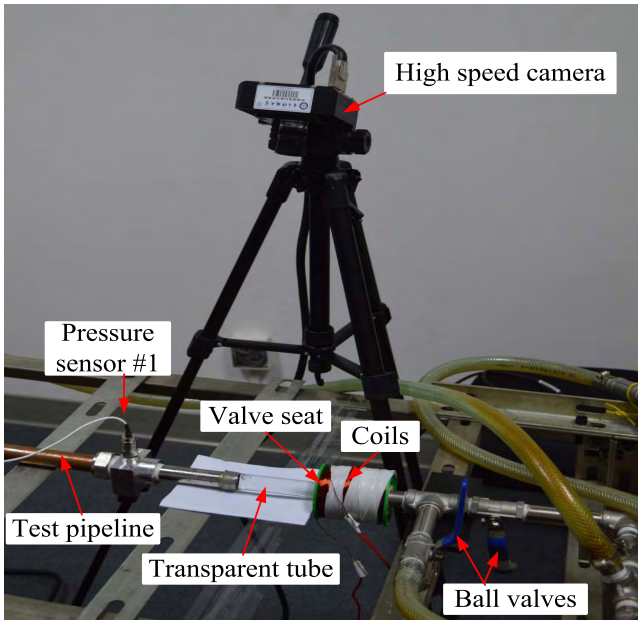

FIGURE 2. The experimental bench of pressure transients.

B. FRICTION MODEL

In the case of turbulent flow, the fluid friction includes the steady friction and the frequency-dependent friction mentioned by Zielke *et al.* [31]. In the momentum equation (2), the friction items which can be approximated as

$$F(q) \approx F_0 + \frac{1}{2}\sum_{i=1}^{k} y_i, \tag{10}$$

where F_0 is the steady friction item for turbulent flow

$$F_0 = \frac{\rho_m f q\,|q|}{4\pi^2 r_0^5}, \tag{11}$$

and k is the number of weighting terms.

Actually, the second sum item of (10) is called frequency-dependent unsteady friction and each y_i can be computed by

$$\begin{cases} y_i(t+\Delta t) = y_i(t)\exp(-n_i\Delta\tau) \\ \qquad\qquad + m_i[q(t+\Delta t) - q(t)]\exp(-n_i\dfrac{\Delta\tau}{2}) \\ y_i(0) = 0, \end{cases} \tag{12}$$

where $i = 1, \ldots k$, n_i and m_i are coefficients of weighting function.

Trikha [32] proposed three exponential weighting items (k=3) to approximate the frequency-dependent friction. Taylor *et al.* [33] optimized the coefficients of Trikha model and proposed a model with four exponential weighting items (k=4). Then Kagama *et al.* [27] modified the error of Trikha model and used an approximate model with ten weighting terms (k=10), which are listed in Table 2.

C. CAVITATION MODEL

Two basic cavitation models include discrete vapor cavity model (DVCM) and discrete gas cavity model (DGCM) [18], [34]. Because the DGCM can only be successfully used with lower initial void fraction($\alpha_i \leqslant 10^{-7}$), the dynamics of the cavitation volume V_{cav} is given by DVCM [2]:

$$\frac{dV_{cav}}{dt} = q_2 - q_1, \tag{13}$$

where q_1 and q_2 are outflow rate and inflow rate at each node, respectively.

TABLE 2. Coefficients of ten weighting terms for Kagama.

i	m_i	n_i	τ_{mi}
1	1.0	2.63744×10^{1}	6.2×10^{-2}
2	1.16725	7.28033×10^{1}	2.8×10^{-2}
3	2.20064	1.87424×10^{2}	9.9×10^{-3}
4	3.92861	5.36626×10^{2}	3.3×10^{-3}
5	6.78788	1.57060×10^{3}	1.1×10^{-3}
6	1.16761×10^{1}	4.61813×10^{3}	3.6×10^{-4}
7	2.00612×10^{1}	1.36011×10^{4}	1.2×10^{-4}
8	3.44541×10^{1}	4.00825×10^{4}	4.1×10^{-5}
9	5.91642×10^{1}	1.18153×10^{5}	1.4×10^{-5}
10	1.01590×10^{2}	3.48316×10^{5}	4.7×10^{-6}

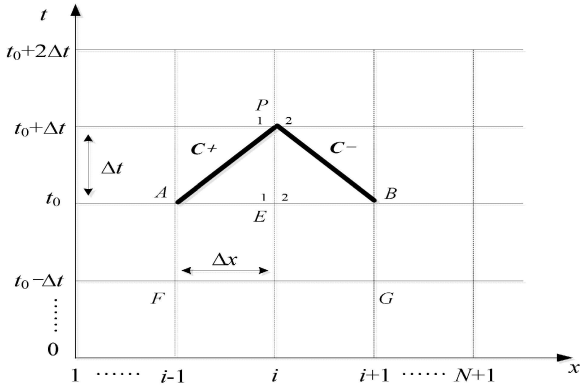

FIGURE 3. The method of characteristics.

IV. SIMULATION METHOD

Based on the mathematical model of transient pressure pulsations as shown in (1∼2), the corresponding simulation is carried out by using method of characteristics(MOC). The continuity equation (1) should be solved together with the momentum equation (2) since they are partial differential forms about the two unknown parameters p and q. Hence, these two partial differential equations can be transformed into the ordinary differential forms along the characteristic lines C^+ and C^- as shown in Fig. 3. The flow rate and pressure are divided into N elements along the pipeline respectively. According to boundary condition, the flow rate in the element around valve is set to be zero and the pressure in the element around the upstream reservoir is constant. Based on the flow rate and pressure at points A and B, the values at point P can be obtained. Subscripts A, B, E, F, G, P indicate different nodes as shown in Fig. 3. See more details about MOC in [1], [2].

From the reference [35] and by using MOC, the number of weighting terms k in (10) can be determined as follow

$$\min(\frac{\Delta\tau_A}{2}, \frac{\Delta\tau_B}{2}) > \tau_{mi}, \tag{14}$$

where

$$\begin{cases} \Delta\tau_A = \dfrac{\Delta x}{2r_0^2 c_0}(\dfrac{\mu_{mA}}{\rho_{mA}} + \dfrac{\mu_{mF}}{\rho_{mF}}) \\ \Delta\tau_B = \dfrac{\Delta x}{2r_0^2 c_0}(\dfrac{\mu_{mB}}{\rho_{mB}} + \dfrac{\mu_{mG}}{\rho_{mG}}). \end{cases} \tag{15}$$

For cavitation model, the cavitation volume at point P in (13) is expressed as:

$$V_{cavP} = V_{cavE} + \frac{\Delta x}{2c_0}(q_{P2} - q_{P1} + q_{E2} - q_{E1}). \tag{16}$$

Two subscripts 1 and 2 are used for left and right limits at each node, respectively.

V. PARAMETRIC IDENTIFICATION

In order to accurately predict the friction item and initial gas bubble volume on pressure transients inside pipelines, genetic algorithms (GAs) for parametric identification are described in this study. There are two sets of pressure data under the same experimental condition obtained by the two pressure sensors. One is used for the model parameter identification by GAs. The other is used to validate the accuracy of model with optimized parameters. The GAs are used to perform a global optimization [36] and obtain the optimal parameters for the frequency-dependent friction model and initial gas bubble volume. For convenience, the fitness function of the proposed GAs is the sum of the errors between the experimental and simulation results.

The coefficients of the weighting terms in (12) are related to the geometric series [16], which can be written as

$$m_i = k_1^{i-1} m_1 (i \geq 2), \tag{17}$$

$$n_i = k_2^{i-1} n_1 (i \geq 2), \tag{18}$$

where k_1 and k_2 are unknown coefficients.

Here the four approximate parameters of the frequency-dependent friction items are identified, i.e., k_1, k_2, m_1, and n_1. To be noted, the initial gas bubble volume is repeatedly identified in different experimental cases. Hence, there are actually five unknown parameters need to be identified. In the GAs optimization, each parameter is binary encoded, and the selection method of the best fitness function is based on roulette, which is minimized by the total errors between the experimental data and predicted pressure pulsations. According to the pressure peaks and its time duration, the fitness function is constructed by evaluating the predicted pressure peaks errors and the predicted peak duration, which can be described as

$$f_f = \sum_j \frac{\int p_{Lth} dt - \int p_{Lexp} dt}{p_{Lss} T_j}, \tag{19}$$

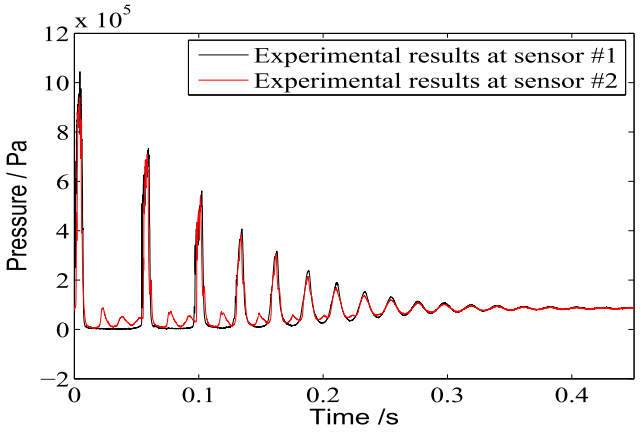

FIGURE 4. The experimental results of pressure pulsations in case 1.

where f_f is the fitness function, p_{Lth} is the predicted pressure results, p_{Lexp} is the experimental pressure data, p_{Lss} is the steady-state pressure, and T_j is the time duration during the experimental pressure peaks.

In the GAs of this study, the number of generations is 1000 and the population size of each generation is 100. Meanwhile, the crossover probability is 0.4 and the mutation probability is 0.005.

VI. EXPERIMENTAL VERIFICATION

The pressure transients with cavitation and gas bubbles are verified under two experimental conditions. The related initial volumes of free gas bubbles in the low pressure water-hydraulic suction pipeline are different in the experimental bench as shown in Fig. 2.

A. CASE 1: A SMALL AMOUNT OF INITIAL GAS BUBBLES EXISTED

A hydraulic filter, that looks like net, is installed at the outlet of the hydraulic return line to reduce initial volume of gas bubbles in water flow. The initial gas bubbles come from the working fluid (water). Deionized water is used as the working fluid. The initial water flow velocity $v_0 = 0.7$ m/s in the experimental pipeline. Fig. 4 shows the comparative results of the pressure pulsations measured by two pressure sensors. When the valve is suddenly shut off at t =0, the first pressure jumps to its maximum pressure value. Then it drops to the vapor pressure and holds this transient value until approximately $t = 0.05$ s. From 0 to 0.2s, there are six pressure peaks. After $t = 0.2$ s, the pressure pulsations becomes an attenuated sinusoidal wave.

The comparative results with Kagama simulation model are shown in Figs. 5-6. There exist obvious differences between the predicted transients with Kagama model and the experimental results, especially in terms of the pressure peak magnitudes and intervals. Therefore, coefficients of the frequency-dependent friction items need to be identified to improve accuracy and adaptability of pressure transient model.

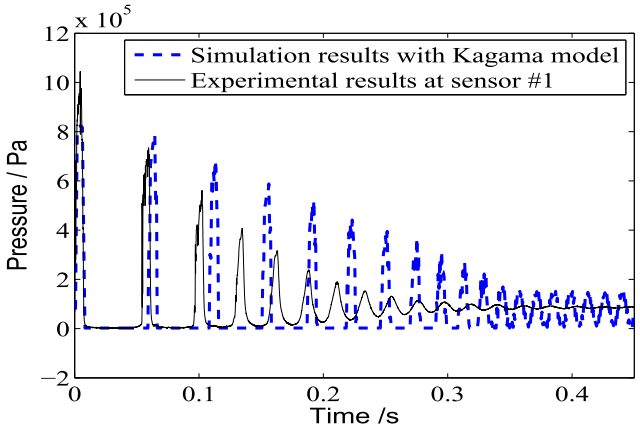

FIGURE 5. The simulation results with Kagama model and experimental results at pressure sensor # 1 in case 1.

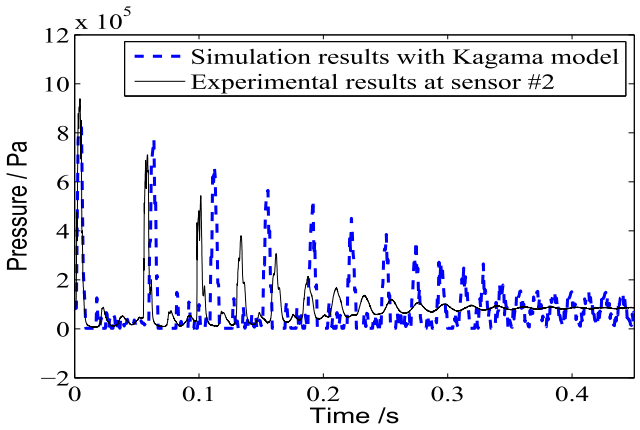

FIGURE 6. The simulation results with Kagama model and experimental results at pressure sensor # 2 in case 1.

Using the pressure data from pressure sensor #1, the proposed GAs have the advantage to search the global optimal parameters of the friction model and initial void fraction (ration of initial gas bubble volume to fluid volume), which are given in Table 3. As both the first four pressure peaks and the time durations between the predicted and experimental results are more concerned, the fitness function covers the only selected periods of the transients(in (19) j is equal to be 4). The model identification results are compared with the corresponding experimental results as shown in Fig. 7. The other pressure data from sensor #2 are used to validate the identified parameters as shown in Fig. 8. It indicates that the proposed parametric identification by GAs has satisfactory consistent performance, especially the first four peaks with high coincident effects of two curves.

Fig. 9 illustrates the growth and collapse sequence of cavitation and bubbles in the tube, which are recorded by the high speed video camera. These images are collected as a movie [37]. In one pressure transient duration, the cavitation and bubbles volume change quickly. The pressure transient video is shown in Video 1 from the supplementary multimedia.

TABLE 3. Identified parameters of the model for case 1.

Identified parameters	Values
k_1	1.055
k_2	1.0696
m_1	1.559
n_1	15.20
α_i	2.089×10^{-5}

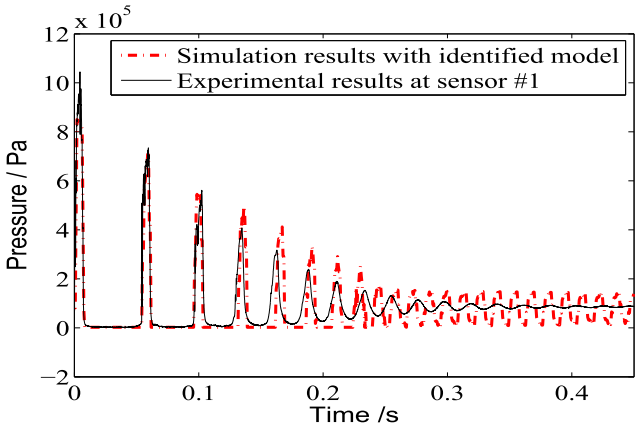

FIGURE 7. The simulation results with the parametric identified model and the experimental results at pressure sensor # 1 in case 1.

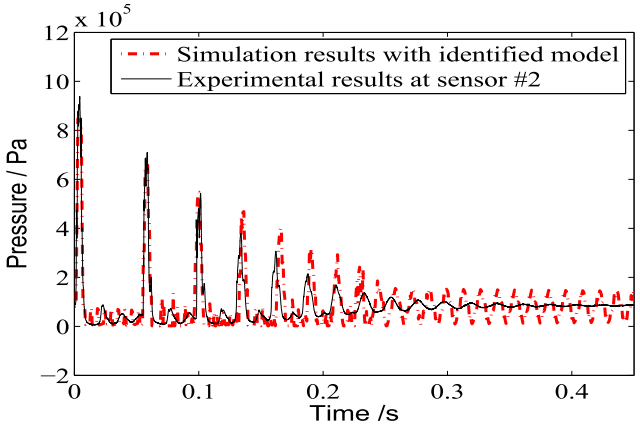

FIGURE 8. The simulation results with the parametric identified model and the experimental results at pressure sensor # 2 in case 1.

The video snapshots of the pressure transients are shown in Figs. 9A-9H. Once the steel ball hits the seat (B), a pressure pulse is created and propagates from the valve to the reservoir. Subsequently, when the pressure drops down to the vapor pressure, it emerges small expanded bubbles and vaporous cavities (C and D). The vaporous cavities are observed to be dispersed on the entire section of the visible tube. Next, as the pressure pulse travels back towards the valve seat, the pressure jumps again and the cavities and gas bubbles collapse (E). Then the pressure drops down again, which leads to cavitation and bubbles again (F). At this moment, the cavities volume was smaller than the former cavities shown in photograph (D). When the third cycle of pressure pulsations finishes, the cavities and bubbles are observed again (G and H).

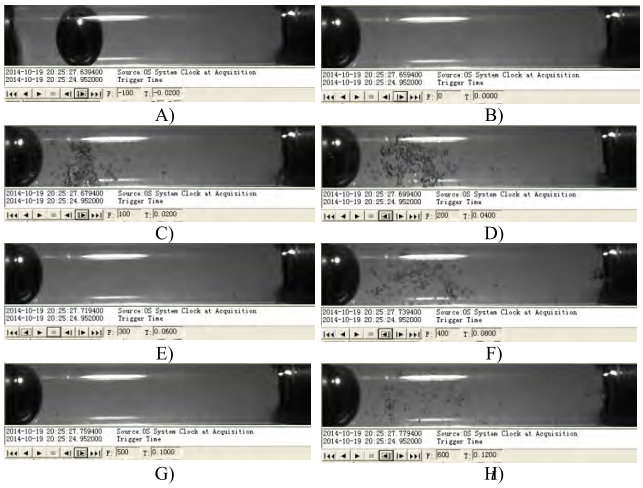

FIGURE 9. The growth and collapse sequence of cavities and bubbles in case 1. (a) t = −0.02 s. (b) t = 0 s. (c) t = 0.02 s. (d) t = 0.04 s. (e) t = 0.06 s. (f) t = 0.08 s. (g) t = 0.1 s. (h) t = 0.12 s.

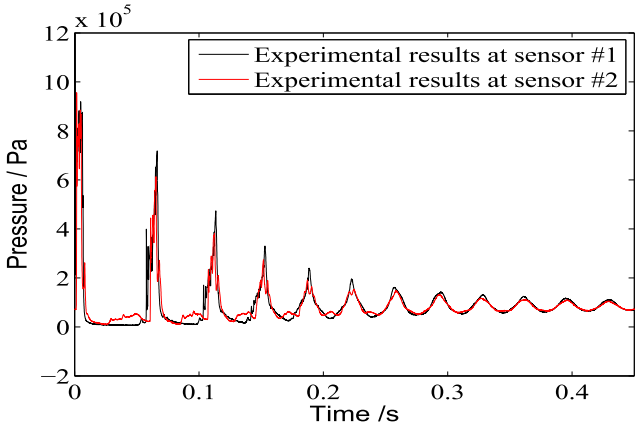

FIGURE 10. The experimental results of pressure pulsations in case 2.

B. CASE 2: MANY INITIAL GAS BUBBLES EXISTED

To further verify the parametric identification model, the second experimental condition with many initial gas bubbles is set up. If the filter is removed from the reservoir, some tiny gas bubbles emerge in the test pipeline. These tiny gas bubbles are mixed evenly with water flow. The experimental pressure transients in case 2 are shown in Fig. 10. The magnitude of the first pressure peak in case 2 is less than that in case 1. Meanwhile, in the duration from 0 to 0.2s, there exist only five pressure peaks in case 2 because the acoustic velocity is decreased with many initial gas bubbles. To be noted that when the initial gas bubbles emerge in water, the magnitudes and numbers of pressure peaks are reduced during the pressure transients.

Similarly, the simulation results with Kagama model and the experimental results of case 2 are shown in Figs. 11-12. Because of coefficients in frequent-dependent friction with Kagama model, unfavorable predicted pressure peaks exist. The predicted pressure pulsations decay slowly and the intervals are larger than the experimental results. In order to improve the predicted transient pressure performance, the uncertain parameters in the model are identified.

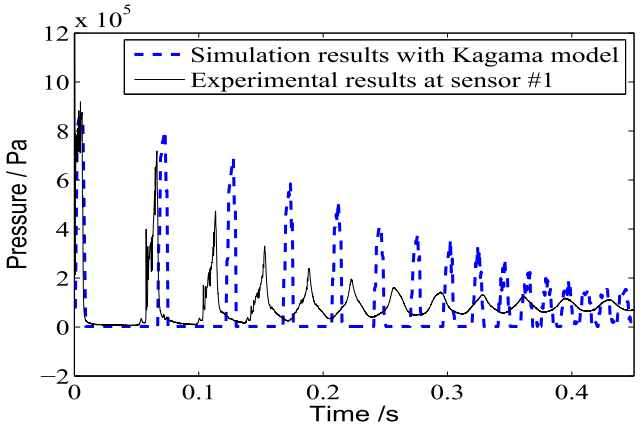

FIGURE 11. The simulation results with Kagama model and experimental results at pressure sensor # 1 in case 2.

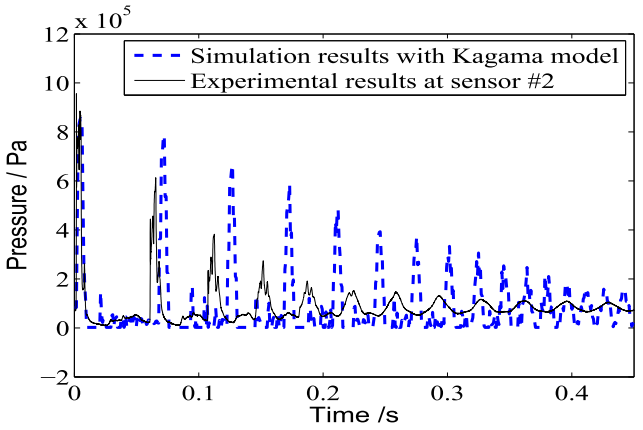

FIGURE 12. The simulation results with Kagama model and experimental results at pressure sensor # 2 in case 2.

For case 2, the initial gas bubble volume is also unknown parameter. However, the weighting function coefficients in frequent-dependent friction model are the same to case 1. Therefore, only the initial gas bubble volume needs to be identified again for case 2. The pressure data from sensor #1 are used for model parameter identification by GAs and other data from sensor #2 for validation. This updated identification of the initial void fraction is 4.088×10^{-5}, which is about twice than that of case 1.

To verify the effectiveness of the parametric identification model, the computed pressure pulsations at the position of pressure sensors #1 and #2 are shown in Figs. 13-14, respectively. Compared with the experimental results of the first four pressure peaks, the values of T_j in (19) are very different for case 1 and case 2. The simulation with parametric identification model has better performance than that with Kagama model, i.e., the magnitudes of the pressure peaks and the intervals have favorable consistency.

Of course, although the general trend of the simulation results are consistent with the experimental pressure pulsations, there still exists certain error after the 4th wave cycle in case 1 and after the 3rd wave cycle in case 2. In the numerical simulation results, at the end of each pressure

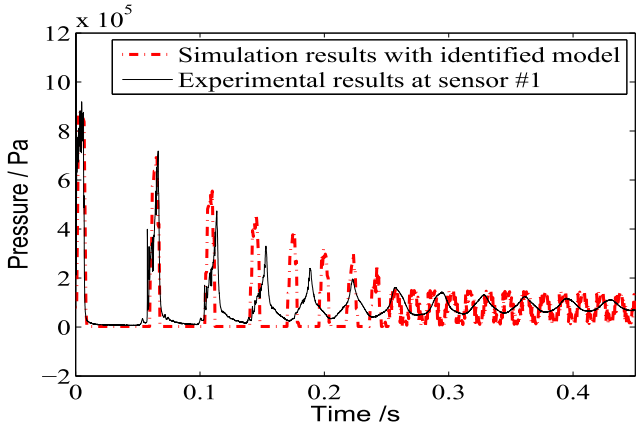

FIGURE 13. The simulation results with the parametric identified model and the experimental results at pressure sensor # 1 in case 2.

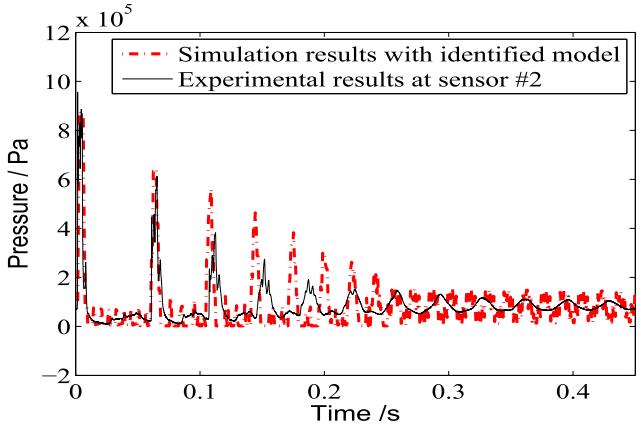

FIGURE 14. The simulation results with the parametric identified model and the experimental results at pressure sensor # 2 in case 2.

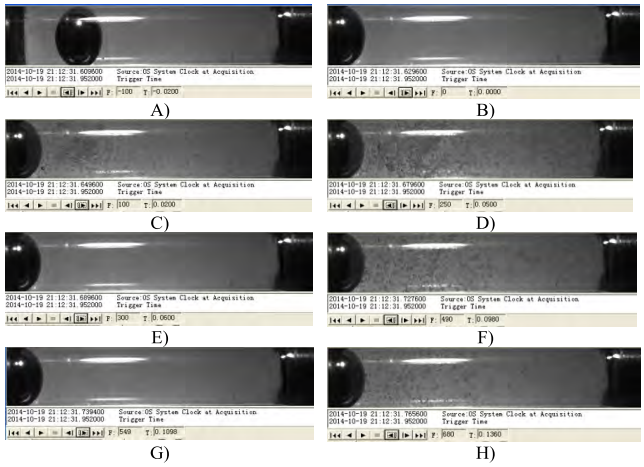

FIGURE 15. The growth and collapse sequence of cavities and bubbles in case 2. (a) t = −0.02 s. (b) t = 0 s. (c) t = 0.02 s. (d) t = 0.05 s. (e) t = 0.06 s. (f) t = 0.098 s. (g) t = 0.1098 s. (h) t = 0.136 s.

transients, high frequency oscillations occur compared with experimental results. These are non-cavitation condition. The experimental results show a characteristic appearance of a lower frequency pressure pulsation after the non-cavitation condition compared with the simulation results. It may be attributed to gas releasing and resolving effects on the acoustic velocity.

The visual results with the cavitation and gas bubbles in case 2 are shown in Fig. 15 and Video 2. The gas bubbles and cavitation near the valve have larger volume than those far from valve (D). However, these cavities are dispersed with smaller volume throughout the water along pipeline in Fig. 15 (D) than that of case 1 shown in Fig. 9 (D). Hence, the gas bubbles in water have a similar effect like springs to absorb the pressure pulsations in case 2.

VII. CONCLUSIONS

A new parametric identification is presented to address unknown frequent-dependent friction model and initial gas bubble volume of pressure transients in water-hydraulic pipelines. The performance index of genetic algorithms is designed as the sum of errors between the simulation and the corresponding experimental results. The comparative results with Kagama model both in simulation and experiment indicate the proposed parametric identification method is feasible to effectively predict the frequent-dependent friction model in water-hydraulic pipeline transients. Future research directions include evaluating the capability of the proposed methodology for coefficients of frequent-dependent friction model and initial gas bubble volume under a large number of different conditions.

Moreover, the effects of gas releasing and resolving are not considered in this paper, that causes the differences between the experimental and simulation results after several wave cycles. In future research, gas releasing and resolving effects can be considered to improve accuracy and robust of pressure transient model.

REFERENCES

[1] E. B. Wylie, L. Suo, and V. L. Streeter, *Fluid Transients in Systems*. Englewood Cliffs, NJ, USA: Prentice-Hall, 1993.
[2] M. H. Chaudhry, *Applied Hydraulic Transients*. New York, NY, USA: Springer, 2014.
[3] Q. Guo, J. Yin, T. Yu, and D. Jiang, "Saturated adaptive control of an electrohydraulic actuator with parametric uncertainty and load disturbance," *IEEE Trans. Ind. Electron.*, vol. 64, no. 10, pp. 7930–7941, Oct. 2017.
[4] Q. Guo, Q. Wang, and Y. Liu, "Antiwindup control of an electrohydraulic system with load disturbance and modeling uncertainty," *IEEE Trans. Ind. Informat.*, vol. 14, no. 7, pp. 3097–3108, Jul. 2018.
[5] Q. Guo, Y. Zhang, B. G. Celler, and S. W. Su, "State-constrained control of single-rod electrohydraulic actuator with parametric uncertainty and load disturbance," *IEEE Trans. Control Syst. Technol.*, vol. 26, no. 6, pp. 2242–2249, Nov. 2018.
[6] W. Shen, J. Wang, H. Huang, and J. He, "Fuzzy sliding mode control with state estimation for velocity control system of hydraulic cylinder using a new hydraulic transformer," *Eur. J. Control*, to be published. doi: 10.1016/j.ejcon.2018.11.005.
[7] Q. Guo, Q. Wang, and X. Li, "Finite-time convergent control of electrohydraulic velocity servo system under uncertain parameter and external load," *IEEE Trans. Ind. Electron.*, vol. 66, no. 6, pp. 4513–4523, Jun. 2019.
[8] Q. Guo, Y. Zhang, B. G. Celler, and S. W. Su, "Neural adaptive backstepping control of a robotic manipulator with prescribed performance constraint," *IEEE Trans. Neural Netw. Learn. Syst.*, to be published. doi: 10.1109/TNNLS.2018.2854699.
[9] W. Shen and J. Wang, "Adaptive fuzzy sliding mode control based on pi-sigma fuzzy neutral network for hydraulic hybrid control system using new hydraulic transformer," *Int. J. Control Autom. Syst.*, to be published. doi: 10.1007/s12555-018-0593-9.

[10] Z. Chen, B. Yao, and Q. Wang, "μ-synthesis-based adaptive robust control of linear motor driven stages with high-frequency dynamics: A case study," *IEEE/ASME Trans. Mechatronics*, vol. 20, no. 3, pp. 1482–1490, Jun. 2015.
[11] Z. Chen, Y.-J. Pan, and J. Gu, "Integrated adaptive robust control for multilateral teleoperation systems under arbitrary time delays," *Int. J. Robust Nonlinear Control*, vol. 26, no. 12, pp. 2708–2728, Aug. 2016.
[12] M. Hirose, *Frequency-Dependent Wall Shear in Transient Fluid Simulation of Unsteady Turbulent Flow*. Boston, MA, USA: MIT, 1972.
[13] K. Suzuki, T. Taketomi, and S. Sato, "Improving Zielke's method of simulating frequency-dependent friction in laminar liquid pipe flow," *J. Fluids Eng.*, vol. 113, no. 4, pp. 569–573, Dec. 1991.
[14] G. A. Schohl, "Improved approximate method for simulating frequency-dependent friction in transient laminar flow," *J. Fluids Eng.*, vol. 115, no. 3, pp. 420–424, Sep. 1993.
[15] A. E. Vardy and J. M. B. Brown, "Transient turbulent friction in fully rough pipe flows," *J. Sound Vib.*, vol. 270, nos. 1–2, pp. 233–257, Feb. 2004.
[16] D. N. Johnston, "Efficient methods for numerical modeling of laminar friction in fluid lines," *J. Dyn. Syst., Meas. Control*, vol. 128, no. 4, pp. 829–834, Mar. 2006.
[17] A. Bergant, A. R. Simpson, and A. S. Tijsseling, "Water hammer with column separation: A historical review," *J. Fluids Struct.*, vol. 22, no. 2, pp. 135–171, 2006.
[18] A. Bergant, A. S. Tijsseling, J. P. Vítkovský, D. I. C. Covas, A. R. Simpson, and M. F. Lambert, "Parameters affecting water-hammer wave attenuation, shape and timing—Part 1: Mathematical tools," *J. Hydraulic Res.*, vol. 46, no. 3, pp. 373–381, 2008.
[19] A. Ferrari, "Modelling approaches to acoustic cavitation in transmission pipelines," *Int. J. Heat Mass Transf.*, vol. 53, no. 19, pp. 4193–4203, 2010.
[20] K. Urbanowicz and Z. Zarzycki, "Improved lumping friction model for liquid pipe flow," *J. Theor. Appl. Mech.*, vol. 53, no. 2, pp. 295–305, 2015.
[21] K. Urbanowicz, "Analytical expressions for effective weighting functions used during simulations of water hammer," *J. Theor. Appl. Mech.*, vol. 55, no. 3, pp. 1029–1040, 2017.
[22] R. Szymkiewicz and M. Mitosek, "Alternative convolution approach to friction in unsteady pipe flow," *J. Fluids Eng.*, vol. 136, no. 1, 2014, Art. no. 011202.
[23] D. Jiang, S. Li, K. A. Edge, and W. Zeng, "Modeling and simulation of low pressure oil-hydraulic pipeline transients," *Comput. Fluids*, vol. 67, pp. 79–86, Aug. 2012.
[24] D. Jiang, S.-J. Li, P. Yang, and T.-Y. Zhao, "Frequency-dependent friction in pipelines," *Chin. Phys. B*, vol. 24, no. 3, Mar. 2015, Art. no. 034701.
[25] N. M. C. Martins, A. K. Soares, H. M. Ramos, and D. I. C. Covas, "CFD modeling of transient flow in pressurized pipes," *Comput. Fluids*, vol. 126, pp. 129–140, Mar. 2016.
[26] N. M. C. Martins, B. Brunone, S. Meniconi, H. M. Ramos, and D. I. C. Covas, "CFD and 1D approaches for the unsteady friction analysis of low Reynolds number turbulent flows," *J. Hydraulic Eng.*, vol. 143, no. 12, Dec. 2017, Art. no. 04017050.
[27] T. Kagawa, I. Lee, A. Kitagawa, and T. Takenaka, "High speed and accurate computing method of frequency-dependent friction in laminar pipe flow for characteristics method," *Trans. Jpn. Soc. Mech. Eng. B*, vol. 49, no. 447, pp. 2638–2644, Jan. 1983.
[28] E. Kojima, M. Shinada, and K. Shindo, "Fluid transient phenomena accompanied with column separation in fluid power pipeline," *Bull. JSME*, vol. 27, no. 233, pp. 2421–2429, Nov. 1984.
[29] A. Adamkowski and M. Lewandowski, "Experimental examination of unsteady friction models for transient pipe flow simulation," *J. Fluids Eng.*, vol. 128, no. 6, pp. 1351–1363, Mar. 2006.
[30] A. Adamkowski and M. Lewandowski, "Investigation of hydraulic transients in a pipeline with column separation," *J. Hydraulic Eng.*, vol. 138, no. 11, pp. 935–944, Nov. 2012.
[31] W. Zielke, H. D. Perko, and A. Keller, "Gas release in transient pipe flow," in *Proc. 6th Int. Conf. Pressure Surges*, Oct. 1989, pp. 3–13.
[32] A. K. Trikha, "An efficient method for simulating frequency-dependent friction in transient liquid flow," *J. Fluids Eng.*, vol. 97, no. 1, pp. 97–105, Mar. 1975.
[33] S. E. M. Taylor, D. N. Johnston, and D. K. Longmore, "Modelling of transient flow in hydraulic pipelines," *Proc. Inst. Mech. Eng., I, J. Syst. Control Eng.*, vol. 211, no. 6, pp. 447–456, 1997.
[34] A. Bergant, A. S. Tijsseling, J. P. Vítkovský, D. I. C. Covas, A. R. Simpson, and M. F. Lambert, "Parameters affecting water-hammer wave attenuation, shape and timing—Part 2: Case studies," *J. Hydraulic Res.*, vol. 46, no. 3, pp. 382–391, Apr. 2010.
[35] J.-J. Shu, "Modelling vaporous cavitation on fluid transients," *Int. J. Pressure Vessels Piping*, vol. 80, no. 3, pp. 187–195, Mar. 2003.
[36] C. Ai, W. Bai, T. Zhang, and X. Kong, "Active control of pressure resonance in long pipeline of bottom founded hydraulic wind turbines based on multi-objective genetic algorithm," *IEEE Access*, vol. 6, pp. 53368–53380, 2018.
[37] A. Adamkowski and M. Lewandowski, "Cavitation characteristics of shutoff valves in numerical modeling of transients in pipelines with column separation," *J. Hydraulic Eng.*, vol. 141, no. 2, Feb. 2015, Art. no. 04014077.

DAN JIANG received the B.E. degree in mechanical engineering and the M.S. and Ph.D. degrees in fluid power transmission and control from the Harbin Institute of Technology, Harbin, China, in 2002, 2005, and 2009, respectively.

Since 2009, she has been with the School of Mechanical and Electrical Engineering, University of Electronic Science and Technology of China, Chengdu, China, where she became a Lecturer. Since 2013, she has been an Associate Professor with the School of Mechanical and Electrical Engineering. From 2014 to 2015, she was an Academic Visitor with the Department of Mechanical and Mechatronics Engineering, University of Waterloo, Canada. She has been a member of the American Society of Mechanical Engineers, since 2012. Her research interests include fluid transmission and control systems, pneumatic systems, and microfluidic technology.

QIXIA LU received the B.E. degree in mechanical engineering from Guizhou University, Guizhou, China, in 2018. She is currently pursuing the M.E. degree with the School of Mechanical and Electrical Engineering, University of Electronic Science and Technology of China. Her current research interests include hydraulic and pneumatic transmission.

YUANMING LIU received the B.E. degree from the School of Advanced Manufacturing Engineering, Chongqing University of Posts and Telecommunications, Chongqing, China, in 2017. He is currently pursuing the M.E. degree with the School of Mechanical and Electrical Engineering, University of Electronic Science and Technology of China. His current research interests include hydraulic and pneumatic transmission.

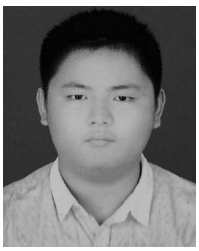

DONGDONG ZHAO received the B.E. degree from the School of Mechanical and Electrical Engineering, University of Electronic Science and Technology of China, in 2018, where he is currently pursuing the M.E. degree. His current research interests include hydraulic and pneumatic transmission.